




BIOSYNTHESIS AND CHARACTERIZATION OF SiO-COCHINEAL DYE NANOPARTICLES BASED ON SALAK FROND SILICA FOR FINGERPRINT VISUALIZATION APPLICATIONS

Sri Adelila Sari*, Feri Yuni Asiyah Kabeakan, and Rani Febriana

Department of Chemistry, Faculty of Mathematics & Natural Sciences, State University of Medan, Indonesia

ARTICLE INFO	ABSTRACT
<p>Keywords: <i>Biosynthesis; Characterization Nanoparticles; Salak Bunch Silica; Cochineal; Fingerprint Visualization.</i></p> <p><i>Article History:</i> Received: 2025-07-23 Accepted: 2025-08-23 Published: 2025-08-31 doi:10.20961/jkpk.v10i2.106785</p>  <p>©2025 The Authors. This open-access article is distributed under a (CC-BY-SA License)</p>	<p>Latent fingerprint visualization is a critical technique in modern forensic science that requires effective and environmentally sustainable coloring agents. This study reports synthesizing and characterizing a novel dyeing agent based on Cochineal insect extract combined with silica derived from salak (<i>Salacca zalacca</i>) bunch waste. It evaluates its application in fingerprint visualization. Cochineal extract was obtained via stepwise heating in a polar solvent, while silica was synthesized through carbonization, demineralization, destruction, and neutralization. The SiO-Cochineal nanoparticles were prepared using a stepwise thermal immobilization method, resulting in covalent bonding between the pigment and silica matrix. Structural and functional group characterization using FTIR confirmed the presence of Si-O-Si, O-H, and C=O groups, indicating successful integration. Application tests on latent fingerprints demonstrated that the composite powders produced sharp and distinct ridge patterns, particularly on non-porous substrates such as glass and optical discs. These findings suggest that SiO-Cochineal-based powders are effective for forensic applications and represent a promising green alternative for latent fingerprint visualization.</p>
<p>*Corresponding Author: sriadelilasari@unimed.ac.id How to cite: S. A. Sari, F. Y. A. Kabeakan, and R. Febriana, "Biosynthesis and Characterization of SiO-Cochineal Dye Nanoparticles Based on Salak Frond Silica for Fingerprint Visualization Applications," <i>Jurnal Kimia dan Pendidikan Kimia (JKPK)</i>, vol. 10, no. 2, pp. 275-294, 2025. [Online]. Available: https://doi.org/10.20961/jkpk.v10i2.106785</p>	

INTRODUCTION

Latent fingerprint identification is one of forensic science's most fundamental and widely applied techniques. It relies on the unique and permanent characteristics of fingerprint ridge patterns, which provide a reliable and tamper-resistant means of personal identification [1], [2]. However, most fingerprints encountered at crime scenes are latent—meaning they are invisible to the naked eye—and therefore require specialized developing agents or dyes to

enable visualization on different porous or non-porous substrates [3].

At present, many of the developing agents employed for latent fingerprint visualization are based on synthetic chemical compounds. While these agents are often effective, they are commonly associated with toxicity, environmental hazards, and potential health risks to forensic practitioners [4]. In line with the increasing emphasis on sustainability and occupational safety, developing visualization agents derived from natural, biodegradable, and environmentally

benign materials has become a critical objective in modern forensic science.

Natural dyes extracted from *Dactylopius coccus* (cochineal insects) represent a promising alternative to synthetic agents. Cochineal produces carminic acid as its primary pigment, a compound extensively applied in the food, pharmaceutical, and cosmetic industries due to its stability against light and temperature and biodegradability [5], [6]. Complementing this, the principles of circular economy and organic waste valorization have highlighted the potential of agricultural byproducts as functional materials. For instance, salacca (*Salacca zalacca*) bunch waste, typically discarded as biomass residue, contains high levels of silica. This silica, characterized by porosity and a high specific surface area, can be an effective carrier and stabilizer for natural dyes [7].

Integrating cochineal pigment with silica derived from salacca waste provides a novel biocomposite approach to developing sustainable fingerprint visualization powders. Importantly, such biosynthesis processes can be carried out through environmentally friendly routes, minimizing toxic solvents and aligning with the principles of green chemistry [8], [9]. To ensure effective application, however, it is essential to characterize the structural and functional interactions within the biocomposite. Fourier Transform Infrared Spectroscopy (FTIR) is particularly suitable for this purpose, as it enables the identification of functional groups, detection of chemical bonding, and analysis of interactions between organic pigments and inorganic carriers [10], [11]

Identifying latent fingerprints is one of the most fundamental techniques in modern forensic science, as it relies on each individual's unique and permanent ridge patterns, making it a reliable and tamper-resistant tool for personal identification [1], [2]. However, most fingerprints recovered from crime scenes are latent or invisible to the naked eye, requiring specific developing agents to visualize them effectively on porous and non-porous substrates [3]. The importance of improving latent fingerprint visualization techniques has become increasingly evident in recent years, as demonstrated by various successful international forensic cases utilizing advanced detection technologies.

Currently, most fingerprint developing agents are based on synthetic chemicals. Although effective, these compounds are often toxic, environmentally unfriendly, and pose health risks to forensic practitioners and ecosystems [4]. Growing awareness of sustainability and occupational safety has emphasized the urgent need for safer, eco-friendly, and natural-based alternatives. This urgency is reinforced by recent findings, such as the documented toxicity of Small Particle Reagents (SPR) [5], the presence of harmful heavy metals in conventional fingerprint powders [6], and safety concerns surrounding cyanoacrylate fuming, which can cause respiratory irritation [7]. Furthermore, the discontinuation of HFE-7100/Novec™ 7100 production by 3M in 2025, along with regulatory restrictions on PFAS in the European Union, further highlights the necessity of developing safer fingerprint visualization agents [8], [9]. These

issues reveal a clear research gap in developing bio-based dye agents that are sensitive and selective across different substrates, safe, environmentally friendly, and supported by toxicological and life-cycle assessments.

Natural dyes extracted from *Dactylopius coccus* (cochineal insects) present promising potential in this context. Cochineal produces carminic acid as its primary pigment, a compound widely used in the food, pharmaceutical, and cosmetic industries due to its thermal, photostability, and biodegradability [5], [6]. Complementing this, the principles of circular economy and agricultural waste valorization encourage using local biomaterials as carriers or stabilizers. Salacca (*Salacca zalacca*) peel waste, long considered an agricultural byproduct, contains a significant amount of silica. With its high porosity and specific surface area, salacca-derived silica can act as an effective matrix to stabilize and immobilize natural dyes [7]. Integrating cochineal pigment with salacca silica into a dye biocomposite provides an innovative approach for developing sustainable and non-toxic fingerprint visualization agents. Importantly, such synthesis can be conducted through green chemistry routes without hazardous solvents, ensuring compatibility with environmental and occupational safety standards.

METHODS

1. Materials

The main equipment used in this study included a furnace (maximum 700°C), a Fourier Transform Infrared (FTIR)

spectrophotometer, a magnetic stirrer with heating capability, a macro camera (smartphone-based), and essential glassware. Specialized forensic tools, including a White Marabou Feather Duster (Sirchie) and Fingerprint Hinge Lifters (Sirchie), were also employed.

The primary materials consisted of cochineal powder, distilled water, concentrated hydrochloric acid (HCl), sodium hydroxide (NaOH, 2 M), potassium bromide (KBr), and porous (black cardboard, wax paper) as well as non-porous substrates (glass slides, aluminum foil, optical discs). A commercial latent fingerprint powder (HI-FI Olcano, Sirchie) was used as a control to compare visualization performance

2. Extraction of Cochineal Powder

Two grams of cochineal powder was extracted with 100 mL of distilled water (solid–liquid ratio 1:50 w/v). The mixture was first heated to 70 °C with continuous stirring for 10 min, followed by heating at 80 °C for an additional 10 min to maximize pigment release. Distilled water was selected as a safe polar solvent for extracting carminic acid, the hydrophilic pigment in cochineal.

3. Synthesis of Silica from Salak Frond Waste

a. Carbonization

Five hundred grams of cleaned and dried Salacca frond waste was carbonized at 500 °C to produce char.

b. Ashing

The char was heated at 700°C for four hours to remove organic matter and concentrate silica. High-temperature

treatment decomposes lignocellulosic components, yielding purer silica, consistent with rice husk and sugarcane bagasse methods.

c. Demineralization

Thirty grams of ash was treated with 300 mL concentrated HCl for 30 min and left for 24 h to dissolve metal impurities (e.g., Ca²⁺, Fe³⁺). The residue was washed with deionized water to neutral pH and dried at 120 °C.

d. Destruction:

Twenty grams of demineralized ash was mixed with 150 mL of 2 M NaOH and boiled for two hours to convert silica into soluble sodium silicate.

e. Gel Formation

The sodium silicate solution was neutralized dropwise with 1 M HCl under stirring until gel formation occurred. The gel was aged for 24 h, washed repeatedly with deionized water until a neutral pH was achieved, dried at 120 °C, and sieved to 200 mesh to obtain uniform silica nanoparticles.

4. Immobilization of Silica–Cochineal Fingerprint Powder Nanoparticles

Four grams of silica nanoparticles were dispersed in 100 mL of cochineal extract and stirred at 60 °C for two hours. Immobilization occurred through hydrogen bonding and electrostatic interactions between the hydroxyl/carboxyl groups of carminic acid and silanol groups on silica. The resulting material was dried at 60 °C and

sieved to 200 mesh to obtain a uniform silica–cochineal nanocomposite powder.

5. Visualization of Latent Fingerprints on Porous and Non-Porous Substrates

Thirty undergraduate participants (Universitas Negeri Medan, batch 2021–2024) provided latent fingerprints by touching their foreheads to deposit natural sebum. Fingerprints were placed on porous (black cardboard, wax paper) and non-porous (glass, aluminum foil, optical discs) surfaces. Visualization was conducted using the dusting method with the synthesized nanocomposite and compared with the commercial Sirchie powder. Ridge clarity was documented with a macro camera, and lift quality was evaluated using standard forensic procedures [13], [14].

6. Characterization of Silica–Cochineal Fingerprint Powder

To characterize the nanocomposite, 1–2 mg of silica–cochineal powder was homogenized with 10 mg KBr to form pellets. FTIR spectra (4000–400 cm⁻¹) were recorded to identify functional groups. Characteristic bands of Si–O–Si (~1100 cm⁻¹), O–H (~3400 cm⁻¹), and C=O (~1650 cm⁻¹) were used as indicators of successful pigment immobilization within the silica matrix.

RESULT AND DISCUSSION

1. Extraction of Cochineal Powder

Extracting pigments from *Dactylopius coccus* (cochineal insects) represents a strategic approach for utilizing biological resources to produce high-value

natural dyes. This study dissolved 2 g of cochineal powder in distilled water (solid–liquid ratio 1:50 w/v), then controlled heating using a magnetic stirrer. The extraction protocol consisted of sequential heating at 70 °C for 10 minutes and 80 °C for another 10 minutes. This controlled temperature regime was intended to maintain carminic acid's stability—the cochineal's primary pigment—while maximizing its release into the polar solvent. Previous studies have confirmed that

the 70–85 °C range is optimal for cochineal pigment extraction without inducing significant thermal degradation [15]–[17].

The resulting filtrate was pinkish-purple (Figure 1), confirming the successful dissolution of carminic acid, an anthraquinone glycoside. Beyond its role as a natural pigment, carminic acid also possesses antioxidant and antimicrobial properties, further expanding its potential applications [18], [19]



Figure 1. Filtrate Resulting from the Extraction of Cochineal Insect Powder

The stability and intensity of the pigment color depend heavily on extraction parameters, especially pH and temperature. Proper control of these factors is essential to ensure consistency and quality of the extract. Continuous stirring during extraction also enhanced the homogeneity of the solution and improved mass transfer, thereby increasing extraction efficiency.

Although conventional heating is effective, more advanced methods such as Ultrasound-Assisted Extraction (UAE) and Microwave-Assisted Extraction (MAE) have

been reported further to improve both the yield and stability of natural pigments. UAE has been shown to increase cochineal pigment yield by 18–22% compared to conventional heating, while MAE can achieve even higher yields of 25–28% within a shorter processing time (5–8 minutes). Moreover, MAE generally produces pigments with better color intensity and fastness, whereas UAE better preserves the molecular integrity of carminic acid by avoiding prolonged exposure to high temperatures [21]–[25]

Table 1. Quantitative comparison of several Cochineal pigment extraction methods

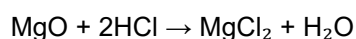
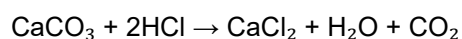
Extraction Method	Operating Temperature	Processing Time	Yield (%)	Pigment Quality
Conventional Heating)	(Gradual 70 – 80 °C	20 min	100 (baseline)	Stable, medium intensity
UAE (Ultrasound-Assisted Extraction)	55–60 °C	15 – 20 min	+18 – 22%	Stable, preserved molecules
MAE (Microwave-Assisted)	60 – 70%	5 – 8 min	+25 – 28%	Higher color intensity, better color fastness

This comparison demonstrates that method selection is a crucial factor in determining pigment yield and quality, which has implications for potential applications of cochineal pigment in various industries, including forensic science

2. Synthesis of Silica from Salak Fronds

The carbonization of 40 g of salacca fronds at 650 °C for 4 hours under limited oxygen produced 16 g of brownish-black ash. This corresponds to a mass reduction of about 40.75%, consistent with the decomposition of lignocellulosic components and the retention of inorganic fractions such as silica, calcium carbonate (CaCO₃), and magnesium oxide (MgO) [24].

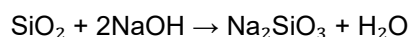
The ash was purified through acid leaching using 4 M HCl for 30 minutes, followed by sedimentation for 24 hours. During this step, metallic impurities such as Ca²⁺ and Mg²⁺ were removed via the following reactions:



Silica (SiO₂), chemically inert to HCl, remained in the solid fraction. After filtration and washing to achieve neutral pH, 11 g of purified ash was obtained. This aligns with

previous reports that strong acid leaching improves silica purity by selectively removing unwanted mineral impurities [26]–[28].

The purified ash was then treated with 1 M NaOH solution to convert silica into soluble sodium silicate according to the reaction:



The solution gradually thickened and darkened, indicating silica dissolution and decomposition of residual carbon. The crude sodium silicate obtained was dissolved in distilled water, soaked for 24 hours, and filtered to remove insoluble residues, yielding a clear sodium silicate solution. Neutralization with 3 M HCl was performed to regenerate silica in gel form:



The resulting white silica gel was aged 24 hours to strengthen its structural framework and porosity. This is consistent with previous findings showing that aging improves silica's morphology and adsorption properties [29]. The gel was washed to neutral pH, dried at 120 °C for 2 hours, and ground into fine powder, yielding 6.53 g of silica with an efficiency of 88% (relative error 11%).

The final product was a white, brittle, fine-textured silica solid, confirming that

salacca fronds can serve as a viable raw material for sustainable silica production.

3. Immobilization of SiO–Cochineal Nanoparticles

Carminic acid ($C_{22}H_{20}O_{13}$), a purplish-red pigment extracted from the insect *Dactylopius coccus* (cochineal), is a bioactive compound with broad potential applications across biotechnology, biosensing, and functional materials. However, its thermal stability and leaching resistance limitations make immobilization approaches crucial to enhance its practical performance [30], [31]. This study investigates the immobilization of carminic acid within a silica matrix derived from salacca frond waste, employing a stepwise thermal synthesis method designed to establish permanent chemical binding.

A total of 4 grams of activated silica obtained from agro-industrial waste was

mixed with 85 mL of cochineal extract solution. The mixing process was conducted at room temperature for one hour using a magnetic stirrer to ensure homogeneous pigment distribution and enhance carminic acid molecules' diffusion into the silica pores [32]. The utilization of silica derived from *Salacca zalacca* fronds has previously been focused mainly on applications such as heavy metal adsorption and catalysis, whereas its use as a matrix for the immobilization of organic pigments has not yet been reported.

Cochineal is recognized for its high color stability but is prone to degradation under light exposure and pH fluctuations. Therefore, the development of silica matrix-based immobilization methods not only has the potential to improve pigment stability but also to extend its applications in forensic science, particularly in the visualization of latent fingerprints on different surfaces



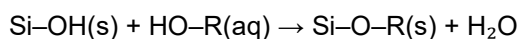
Figure 2. Homogenization process of silica and cochineal solution using a magnetic stirrer.

Silica was selected as the immobilization matrix due to its favorable characteristics, including high biocompatibility, large specific surface area, and surface silanol groups ($-Si-OH$). These functional groups enable initial interactions through hydrogen bonding, van der Waals forces, and electrostatic attraction with the

hydroxyl groups of carminic acid. However, such non-covalent interactions alone are insufficient to ensure long-term stability. Therefore, the formation of covalent bonds between the pigment and silica is necessary to enhance resistance to leaching and chemical degradation [33].

The synthesis was carried out through a stepwise thermal treatment. The first stage involved heating at 60 °C for one hour to promote pigment adsorption onto the silica surface and partially evaporate the solvent. This process reduces solvent competition for reactive sites and creates optimal conditions for direct interaction between the hydroxyl groups of the pigment and the silanol groups on the silica surface [34].

The second stage involved heating at 150 °C for one hour to initiate a condensation reaction that resulted in covalent Si–O–C bonds forming. The primary reaction can be described as follows:



Where *R* represents the aromatic structure of carminic acid, this reaction releases water as a by-product and establishes an irreversible covalent bond (Zhao et al., 2024). This mechanism is consistent with covalent bonding behavior reported in other metal oxide systems, such as Ti–O–Si and Al–O–C, which have been shown to improve the structural stability of hybrid materials [35], [36].

The transformation resulting from this thermal treatment produced a purplish-red powder with high visual and functional stability. Water leaching tests confirmed that the pigment remained strongly bound to the silica matrix, thereby verifying the successful formation of covalent bonds (Figure 3)



Figure 3. Pigment powder resulting from the immobilization process.

Using agro-industrial waste as a silica source provides added value from both sustainability and circular economy perspectives. Beyond improving process efficiency, this approach reinforces the study's relevance within the green chemistry framework. Furthermore, the resulting silica can be engineered through pore-size modification, surface functionalization, or

metal ion incorporation to develop more selective and multifunctional dye systems. Potential applications extend beyond water-based textiles, including color-change-based optical sensors and pH indicators [37], [38].

Overall, the findings of this study demonstrate that immobilizing carminic acid onto silica surfaces via thermal synthesis is an effective strategy to produce natural-

based solid dyes with enhanced durability. Temperature and time control during thermal treatment were critical parameters for optimizing covalent bond formation and material stability. These results pave the way for developing adaptive and sustainable functional materials based on natural pigments, aligned with future technological demands [39], [40].

4. Visualization of Fingerprint Powder

Latent fingerprint visualization is a critical technique in forensic identification, as it allows investigators to reveal trace evidence that is typically invisible to the naked eye. In this study, the powder dusting method was employed to detect latent fingerprints across different types of surfaces.

The participants were randomly selected undergraduate students from Universitas Negeri Medan, class of 2021–2024. Before fingerprint collection, participants were instructed to wash their hands thoroughly to eliminate contaminants that could interfere with visualization quality [41]–[43].

Handwashing with soap followed by natural air drying was intended to remove external residues while allowing natural sebum secretion. Sebum plays a vital role in fingerprint deposition because it acts as an adhesive medium that enhances the clarity of ridge patterns when transferred onto a substrate. Previous studies have emphasized that sebum increases the density and adhesion of fingerprint residues, thereby improving the likelihood of successful development of latent patterns [44].

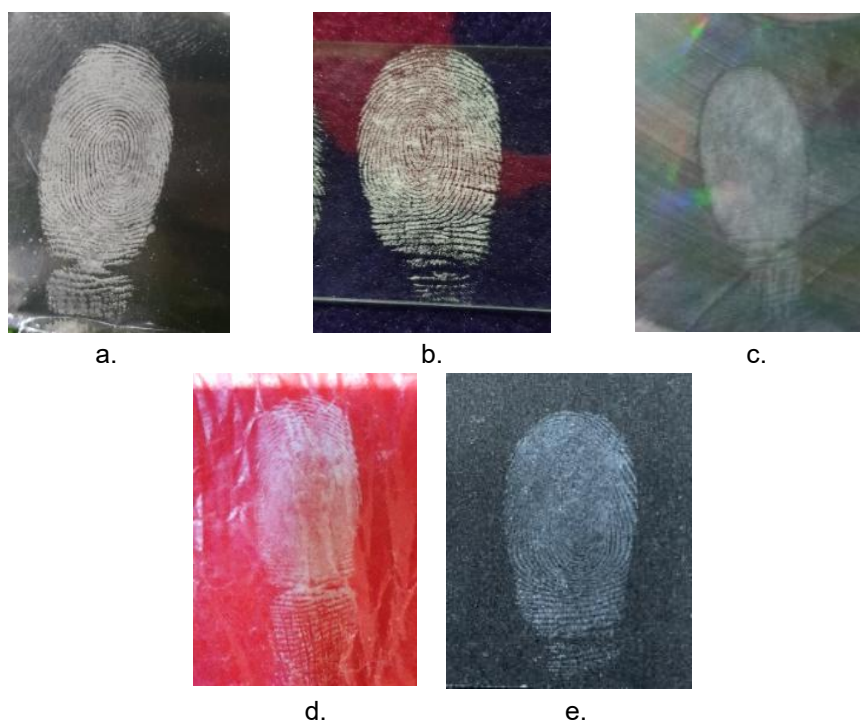


Figure 4. Visualization of Latent Fingerprints Using SiO–Cochineal Nanoparticle Powder: (a) Aluminum Foil; (b) Microscope Slide; (c) CD; (d) Wax Paper; (e) Cardboard

Fingerprints were deposited onto both non-porous and porous surfaces. The

non-porous substrates included microscope slides, compact discs (CDs), and aluminum

foil, while the porous substrates comprised wax paper and cardboard. The choice of these materials was essential for evaluating the dusting method's performance, since each substrate's physical properties strongly influence visualization quality. Prior research has consistently demonstrated that non-porous surfaces retain powder particles more effectively, producing sharper and more well-defined ridge details [45], [46].

After applying the synthesized powder, ridge patterns became distinctly visible. The method proved especially effective on substrates where strong interactions occurred between the fingerprint

oils and the powder particles [47], as illustrated in Figure 4.

The results showed significant variation in clarity and sharpness of fingerprint patterns depending on the powder type and surface characteristics. Figure 5 presents a comparative chart of the clarity and sharpness scores of fingerprint patterns across different surfaces to strengthen these findings. Non-porous substrates such as microscope slides and CDs achieved the highest scores, demonstrating their effectiveness in preserving papillary ridge details.

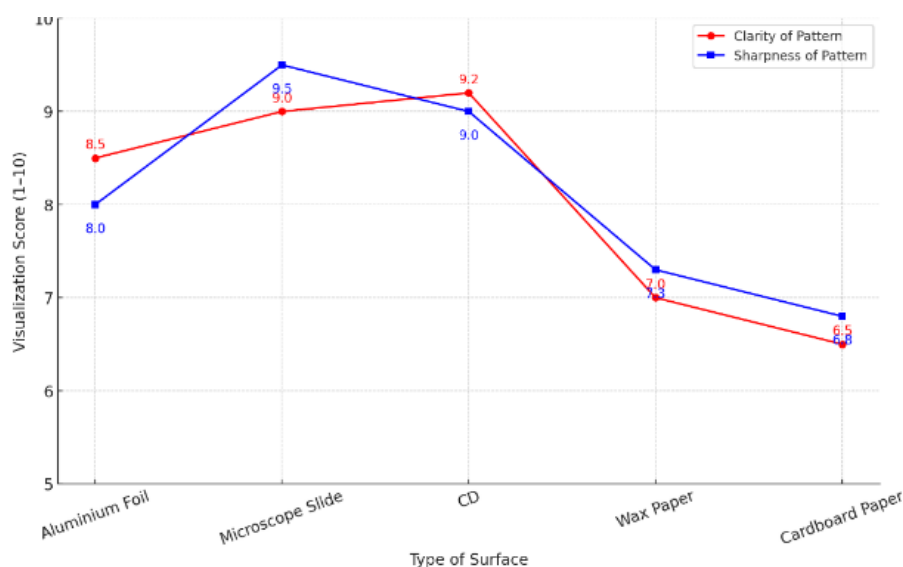


Figure 5. Comparative Clarity and Sharpness Scores of Fingerprints on Various Surface Types.

Previous research has noted that nanosized powders, such as fluorescent nanoparticles, provide higher contrast and more precise ridge detail on porous and non-porous surfaces [6]. For instance, chemically modified carbon or zinc oxide nanoparticles have been shown to enhance visualization results compared to conventional powders.

Moreover, this study supports the development of alternative natural-based materials as fingerprint-revealing agents that are more environmentally friendly. Using organic materials, such as dried flower powder or natural extracts, is considered a safer and effective approach to improving visualization performance [48]. These

findings align with the growing movement in green forensics, which emphasizes sustainability in forensic laboratory practices. Several factors influence the interaction dynamics between powders and fingerprint residues, including particle size, material polarity, and surface roughness. Recent studies have shown that smaller particle sizes result in better development due to increased surface contact area and improved adhesion [49].

Regarding visualization technology, advances in fluorescence techniques and digital image processing have expanded the capabilities for detecting latent fingerprints. These innovations have improved accuracy and revealed microscopic details of ridge patterns, even in prints exposed to environmental degradation or contamination. Such methods demonstrate significant potential for application in modern forensic practice [50].

This study reinforces that powder dusting remains a relevant and effective technique, particularly when combined with modern materials and visualization approaches. It offers a simple yet reliable method for revealing latent fingerprint patterns. Considering innovations in material selection and visualization technology, this technique has the potential to serve as a key tool in current and future forensic investigation and law enforcement systems [47].

5. Characterization of Powder Using FTIR

Functional group characterization of the SiO–Cochineal sample was performed

using Fourier Transform Infrared (FTIR) spectroscopy to identify the functional groups involved in the biosynthesis process and to analyze the interactions between silica (SiO₂) and the active compounds present in the cochineal extract. The FTIR spectrum, recorded in the range of 4000–400 cm⁻¹, revealed several absorption peaks of significant importance regarding the composition and molecular interactions within the system. This spectral analysis confirmed silica as the major component of the sample while also providing evidence for the presence of carmine, the primary pigment derived from *Dactylopius coccus* [51].

The most prominent absorption peaks were observed at 1062.541 cm⁻¹, 795.608 cm⁻¹, and 445.782 cm⁻¹, corresponding to asymmetric stretching vibrations of Si–O–Si, symmetric stretching of Si–O–Si, and bending vibrations of O–Si–O, respectively. These bands confirm the dominance of silica in the nanoparticle structure, which is consistent with previous studies highlighting the characteristic absorption behavior of silica-based materials [52]. The green biosynthesis approach applied in this study is also suggested to contribute to the unique functional characteristics of the synthesized material.

Two broad absorption peaks indicated the presence of carmine within the system (Figure 6). The first, at 1629.396 cm⁻¹, is primarily associated with O–H bending vibrations, which may be attributed to adsorbed water. However, this band may also include contributions from carbonyl (C=O) and/or double bond (C=C) stretching within the anthraquinone backbone of

carminic acid (Mahardika et al., 2021). The second broad absorption peak, observed at 3366.840 cm^{-1} , corresponds to O–H stretching vibrations, arising from both adsorbed water and phenolic hydroxyl groups present in carminic acid—the active component of carmine. Previous studies have reported that O–H stretching in silica-based systems may also indicate the

presence of other adsorbed species, which supports the multifunctional interaction observed in this material [53].

To complement the spectral data, Table 2 summarizes the major FTIR absorption peaks identified in the SiO–Cochineal fingerprint powder sample and their corresponding wavenumbers and functional group assignments.

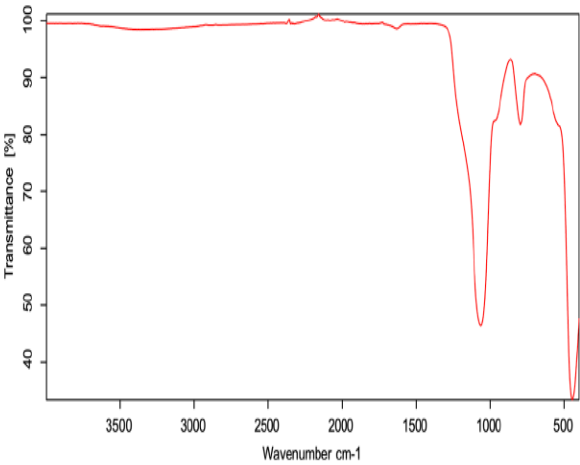


Figure 6. FTIR Spectrum of Cochineal–Silica Fingerprint Powder

Table 2. FTIR Absorption Peaks of the Fingerprint Powder Sample

Wavenumber (cm ⁻¹)	Abs. Intensity	Rel. Intensity	Width	Threshold	Shoulder
3366.84	0.983	0.015	1071.71	1.65	0
2348.614	0.993	0.01	65.204	1.37	0
1629.396	0.985	0.013	89.156	1.37	0
1062.541	0.465	0.48	129.09	68.99	0
795.608	0.817	0.104	52.217	13.11	0
445.782	0.334	0.143	53.48	19.1	0

The infrared spectrum revealed several significant peaks, reflecting the presence of principal functional groups and chemical interactions within the silica-based material system. The absorption band at 3366.840 cm^{-1} (absolute intensity: 0.983; relative intensity: 0.015) corresponds to O–H stretching vibrations. This band is strongly associated with adsorbed water on the silica

surface or hydroxyl groups inherently present in the silica structure. These findings are consistent with previous reports identifying this spectral region as a typical marker of O–H vibrations in silica-based materials [54], [55]. Moreover, the interaction between adsorbed water and silica surfaces has significantly influenced O–H vibrational

dynamics, thereby modifying spectral characteristics [56].

The absorption peak at 2348.614 cm^{-1} (absolute intensity: 0.993; relative intensity: 0.010) is attributed to the stretching vibrations of $\text{C}\equiv\text{O}$ or $\text{C}\equiv\text{N}$ groups, commonly associated with atmospheric carbon dioxide (CO_2) adsorbed onto the sample. Although this peak may represent a measurement artifact, its presence is still relevant as it indicates potential CO_2 interactions with the porous silica matrix. Previous studies have reported that CO_2 molecules can become physically adsorbed or trapped in porous systems, thereby contributing to spectral features in this region [57].

Another distinct absorption band was observed at 1629.396 cm^{-1} (absolute intensity: 0.985; relative intensity: 0.013), corresponding to O–H bending vibrations, further confirming the presence of adsorbed water. In the case of cochineal-containing systems, such as the SiO–Cochineal composite analyzed in this study, this band may also be associated with C=O stretching in carbonyl groups or C=C stretching vibrations within the anthraquinone backbone of carminic acid. Absorption peaks in this region often indicate water adsorption capacity and the structural integrity of silica-based composites [58], [59].

The dominant absorption peak at 1062.541 cm^{-1} (absolute intensity: 0.465; relative intensity: 0.480) is characteristic of asymmetric Si–O–Si stretching vibrations, confirming silica (SiO_2) as the primary component of the material. This assignment is consistent with earlier studies, which identified this band as a reliable marker for

both amorphous and crystalline silica frameworks [60], [61].

Additionally, the bands at 795.608 cm^{-1} and 445.782 cm^{-1} correspond to symmetric stretching of Si–O–Si and bending vibrations of O–Si–O, respectively. These peaks reinforce the conclusion that silica is the dominant constituent of the synthesized material. Similar findings have been reported in silica characterization studies, which emphasized the importance of these features in assessing the homogeneity and structural stability of silica-based systems [62], [63].

To provide further clarity regarding these interactions, Table 3 compares the FTIR peaks of pure silica, pure cochineal extract, and the synthesized SiO–Cochineal composite. The observed shifts, particularly in the O–H, C=O, and Si–O–Si regions, suggest strong chemical interactions and possible covalent bond formation between silica and the active compounds of cochineal.

The FTIR data comparison in Table 2 shows that the SiO–Cochineal composite undergoes noticeable absorption peak shifts compared to pure silica and pure cochineal. The most pronounced shifts are observed in the asymmetric Si–O–Si stretching region, shifting from $1080\text{--}1090\text{ cm}^{-1}$ to 1062.54 cm^{-1} , and in the O–H stretching region, shifting from approximately 3450 cm^{-1} to 3366.84 cm^{-1} . These shifts indicate strong interactions—through both hydrogen bonding and possible partial covalent bonding—between the hydroxyl groups of silica and the phenolic/carbonyl groups of carminic acid in cochineal.

In addition, small shifts in the symmetric Si–O–Si stretching and O–Si–O bending peaks suggest structural modifications within the silica framework due to the incorporation of organic molecules. This spectral evidence supports the conclusion that the green biosynthesis process results in the physical attachment of carmine pigment to the silica

surface and in the formation of stable chemical interactions. Such integration of organic–inorganic compounds is expected to enhance the material's functional properties, including stability and effectiveness in forensic applications such as latent fingerprint visualization.

Table 3. Comparison of FTIR peaks of pure silica, pure cochineal, and SiO–Cochineal composite.

Functional Group / Vibration Mode	Pure Silica (cm ⁻¹) [Ref]	Pure Cochineal (cm ⁻¹) [Ref]	SiO–Cochineal Composite (cm ⁻¹)	Shift & Interpretation
O–H stretching	~3450 [54]	3370–3400 [53]	3366.84	Slight shift; indicates possible hydrogen bonding between silica hydroxyl groups and carminic acid phenolic hydroxyl groups.
C=O / C=C stretching	-	1630 – 1650 [60]	1629.40	Minimal shift; suggests interaction between carbonyl/aromatic groups and the silica surface
Asymmetric Si–O–Si stretching	1080–1090 [60]	-	1062.54	Shift to lower wavenumber; indicates interaction or partial covalent bond formation with cochineal organic molecules.
Symmetric Si–O–Si stretching	~800 [62]	-	795.61	Slight shift; indicates silica framework modification by organic molecules.
O – Si – O bending	~460 [63]	-	445.78	Slight shift; possible bond angle changes due to organic compound integration into the silica structure

The infrared spectral analysis confirms that FTIR spectroscopy is a reliable technique for identifying major functional groups and molecular interactions in silica–organic systems, including contributions from adsorbed water and atmospheric gases. The observed peak shifts further demonstrate that infrared spectroscopy provides valuable structural insights while also enabling evaluation of the potential applications of such composite materials in engineering and forensic domains [64], [65].

CONCLUSION

This study successfully developed a dyeing agent based on a combination of cochineal insect extract and silica derived from salak peel waste, which proved effective for visualizing latent fingerprints. The biosynthesis process yielded stable and homogeneous SiO–Cochineal nanoparticles, with functional structures confirmed through FTIR spectroscopy. The main absorption peaks indicated the presence of silica and carmine pigment functional groups, chemically interacting and reinforcing the bonding between inorganic and organic components. Visualization tests demonstrated that the powder performed

best on non-porous surfaces while maintaining satisfactory results on porous substrates. These findings highlight the significant potential of biomass waste-based materials and natural dyes for applications in sustainable forensics. Moving forward, this approach can be further enhanced by exploring other local biomaterials, surface functionalization, and integrating digital visualization technologies to improve sensitivity and accuracy in identification applications.

ACKNOWLEDGEMENT

The authors would like to express their sincere gratitude to the Institute for Research and Community Service (LPPM), Universitas Negeri Medan (Unimed), for the valuable funding and facilitation provided under the Rector's Decree No. 0194/UN33/KPT/2025. This support has enabled the successful implementation of the research and community engagement activities from start to finish.

REFERENCES

- [1] I.K., A. M., S. J. Monica, and S. C., "Antioxidant and antimicrobial activities of silver and iron nanoparticles synthesized from jackfruit peel (*Artocarpus heterophyllus*): A sustainable waste valorization approach," *Environment and Ecology*, vol. 43, no. 2, pp. 375–384, Apr. 2025, doi: [10.60151/envec/trpp7406](https://doi.org/10.60151/envec/trpp7406)
- [2] S. Javed, A. Ali, S. Alam, M. Rafique, B. Gul, H. J. Chaudhary, and E. Y. Santali, "Biosorption of cadmium and chromium from wastewater using *Bacillus xiamenensis* and *Bacillus cereus* isolated from the sugarcane rhizosphere," *ACS ES&T Water*, vol. 4, no. 9, pp. 4140–4149, 2024, doi: [10.1021/acsestwater.4c00406](https://doi.org/10.1021/acsestwater.4c00406).
- [3] A. Samy, A. M. Ismail, and H. Ali, "Environmentally friendly mesoporous SiO₂ with mixed fiber/particle morphology and large surface area for enhanced dye adsorption," *J. Mater. Sci.*, vol. 58, no. 4, pp. 1586–1607, Jan. 2023, doi: [10.1007/s10853-022-08119-2](https://doi.org/10.1007/s10853-022-08119-2).
- [4] Q. Ain Leghari *et al.*, "Eco-friendly synthesis of silver nanoparticles from pomegranate peel extract and their antibacterial activity," *Kashf Journal of Multidisciplinary Research*, no. 1, pp. 2–4, 2025. [Online]. Available: <https://kjmr.com.pk>
- [5] V. Singh *et al.*, "Heavy metal contamination in the aquatic ecosystem: Toxicity and its remediation using eco-friendly approaches," *Toxics*, Feb. 2023, doi: [10.3390/toxics11020147](https://doi.org/10.3390/toxics11020147).
- [6] P. S. Penteado *et al.*, "Green extraction and NMR analysis of bioactives from orange juice waste," *Foods*, vol. 14, no. 4, Feb. 2025, doi: [10.3390/foods14040642](https://doi.org/10.3390/foods14040642).
- [7] I. Degli Esposti, L. Guerrisi, G. Peruzzi, S. Giulietti, and D. Pontiggia, "Cell wall bricks of defence: The case study of oligogalacturonides," *Front. Plant Sci.*, 2025, doi: [10.3389/fpls.2025.1552926](https://doi.org/10.3389/fpls.2025.1552926).
- [8] I. Vicente-Zurdo, E. Gómez-Mejía, S. Morante-Zarcero, N. Rosales-Conrado, and I. Sierra, "Analytical strategies for green extraction, characterization, and bioactive evaluation of polyphenols, tocopherols, carotenoids, and fatty acids in agri-food bio-residues," *Molecules*, Mar. 2025, doi: [10.3390/molecules30061326](https://doi.org/10.3390/molecules30061326).
- [9] J. Sandhya and M. Neelamegam, "Biosynthesis of nanoparticles from bio waste and its application on anti-corrosion, antifungal and paint

- applications," *Int. J. Sci. Res. Eng. Manag.*, vol. 9, no. 4, 2025, doi: [10.55041/ijserem44611](https://doi.org/10.55041/ijserem44611).
- [10] I.J. Horst, C. A. Duvosin, and R. D. A. Vieira, "Synthesis of 2D heterostructures: MoS₂/GO and MoS₂/graphene via microdrop and CVD deposition," *Int. J. Nanosci.*, vol. 20, no. 6, pp. 1–8, 2021, doi: [10.1142/S0219581X21500502](https://doi.org/10.1142/S0219581X21500502).
- [11] W. Yeddes et al., "Optimization of phenolic compound extraction from Tunisian squash by-products: A sustainable approach for antioxidant and antibacterial applications," *Open Life Sci.*, vol. 20, no. 1, Jan. 2025, doi: [10.1515/biol-2025-1096](https://doi.org/10.1515/biol-2025-1096).
- [12] T. S. Echegaray-Ugarte et al., "Green synthesis of silver nanoparticles mediated by *Punica granatum* peel waste: An effective additive for natural rubber latex nanofibers enhancement," *Polymers (Basel)*, vol. 16, no. 11, Jun. 2024, doi: [10.3390/polym16111531](https://doi.org/10.3390/polym16111531).
- [13] S. A. Sari and D. H. Nasution, "Development of nail henna (*Lawsonia inermis* Linn.) leaf powder as a latent fingerprint visualization on non-porous and porous surfaces," *J. Med. Chem. Sci.*, vol. 6, no. 3, pp. 540–552, Mar. 2023, doi: [10.26655/jmchemsci.2023.3.11](https://doi.org/10.26655/jmchemsci.2023.3.11).
- [14] S. A. Sari and D. H. Nasution, "Pengembangan metode serbuk daun suji (*Pleomele angustifolia* N.E.Br) sebagai identifikasi sidik jari laten," *Jurnal Riset Kimia*, vol. 12, no. 2, Sep. 2021, doi: [10.25077/jrk.v12i2.406](https://doi.org/10.25077/jrk.v12i2.406).
- [15] B. Do and H. Kwon, "Genotoxicity test of eight natural color additives in the Korean market," *Genes Environ.*, vol. 44, no. 1, Dec. 2022, doi: [10.1186/s41021-022-00247-0](https://doi.org/10.1186/s41021-022-00247-0).
- [16] R. Reyes-Pérez et al., "Cochineal (*Dactylopius coccus* Costa) pigment extraction assisted by ultrasound and microwave techniques," *Molecules*, vol. 29, no. 23, Dec. 2024, doi: [10.3390/molecules29235568](https://doi.org/10.3390/molecules29235568).
- [17] R. Karadag, "Cotton dyeing with cochineal by just in time extraction, mordanting, dyeing, and fixing method in the textile industry," *J. Nat. Fibers*, vol. 20, no. 1, pp. 1–11, 2023, doi: [10.1080/15440478.2022.2108184](https://doi.org/10.1080/15440478.2022.2108184).
- [18] H. P. Melo, A. J. Cruz, J. Sanyova, S. Valadas, and A. M. Cardoso, "Paint, colour, and style: The contribution of minerals to the palette of *The Descent from the Cross*, attributed to the Portuguese painter Francisco João (act. 1558–1595)," *Minerals*, vol. 13, no. 9, Sep. 2023, doi: [10.3390/min13091182](https://doi.org/10.3390/min13091182).
- [19] A. Pasdaran, M. Zare, A. Hamed, and A. Hamed, "A review of the chemistry and biological activities of natural colorants, dyes, and pigments: Challenges, and opportunities for food, cosmetics, and pharmaceutical application," *Chem. Biodivers.*, vol. 20, no. 8, 2023, doi: [10.1002/cbdv.202300561](https://doi.org/10.1002/cbdv.202300561).
- [20] I. Celis, C. Segura, J. S. Gómez-Jeria, M. Campos-Vallette, and S. Sanchez-Cortes, "Analysis of biomolecules in cochineal dyed archaeological textiles by surface-enhanced Raman spectroscopy," *Sci. Rep.*, vol. 11, no. 1, Dec. 2021, doi: [10.1038/s41598-021-86074-9](https://doi.org/10.1038/s41598-021-86074-9).
- [21] K. Sutor-Świeży et al., "*Basella alba* L. (Malabar spinach) as an abundant source of betacyanins: Identification, stability, and bioactivity studies on natural and processed fruit pigments," *J. Agric. Food Chem.*, vol. 72, no. 6, pp. 2943–2962, Feb. 2024, doi: [10.1021/acs.jafc.3c06225](https://doi.org/10.1021/acs.jafc.3c06225).
- [22] S. Sankararaman, "Phase portrait and fractal analyses in nanobiophotonics: Carbon nanoparticle aided intra-pigment

energy transfer in leaves," *Phys. Scr.*, vol. 97, no. 6, 2022.

- [23] R. Kiruthiga and G. Thiruneelakandan, "Isolation and identification of pigments from marine actinomycetes, along with their potential applications," *J. Adv. Zool.*, vol. 44, no. 4, pp. 869–876, Nov. 2023, doi: [10.17762/jaz.v44i4.2209](https://doi.org/10.17762/jaz.v44i4.2209).
- [24] S. Yuan, Y. Hou, S. Liu, and Y. Ma, "A comparative study on rice husk, as agricultural waste, in the production of silica nanoparticles via different methods," *Materials*, vol. 17, no. 6, Mar. 2024, doi: [10.3390/ma17061271](https://doi.org/10.3390/ma17061271).
- [25] I. Wei, S. H. Urashima, S. Nihonyanagi, and T. Tahara, "Elucidation of the pH-dependent electric double layer structure at the silica/water interface using heterodyne-detected vibrational sum frequency generation spectroscopy," *J. Am. Chem. Soc.*, vol. 145, no. 16, pp. 8833–8846, Apr. 2023, doi: [10.1021/jacs.2c11344](https://doi.org/10.1021/jacs.2c11344).
- [26] A.G. Setyadi and S. H. Widiyarti, "Analisis tekanan darah karyawan sebelum dan sesudah melakukan pekerjaan di ketinggian pada PT. Chandra Asri Petrochemical Site Office Serang," *Jurnal Ners Universitas Pahlawan*, vol. 7, no. 2, pp. 9630–968, 2023. doi: [10.31004/jn.v7i2.16022](https://doi.org/10.31004/jn.v7i2.16022).
- [27] Irzaman, D. Yustaeni, Aminullah, Irmansyah, and B. Yulianto, "Purity, morphological, and electrical characterization of silicon dioxide from cogon grass (*Imperata cylindrica*) using different ashing temperatures," *Egypt. J. Chem.*, vol. 64, no. 8, pp. 4143–4149, Aug. 2021, doi: [10.21608/ejchem.2019.15430.1962](https://doi.org/10.21608/ejchem.2019.15430.1962).
- [28] P. Nurjanto, K. Khamidinal, I. Fajriyati, and D. Krisdiyanto, "Sintesis silika gel dari pelepah pohon salak pondoh dengan metode sol-gel menggunakan NaOH dan HCl," *Indonesian Journal of Materials Chemistry*, vol. 3, no. 2, 2020, doi: [10.14421/ijmc.v3i2.3913](https://doi.org/10.14421/ijmc.v3i2.3913).
- [29] D. Shandurkov, N. Danchova, T. Spassov, V. Petrov, R. Tsekov, and S. Gutzov, "Silica gels doped with gold nanoparticles: Preparation, structure and optical properties," *Gels*, vol. 9, no. 8, Aug. 2023, doi: [10.3390/gels9080663](https://doi.org/10.3390/gels9080663).
- [30] U. G. Longo *et al.*, "Biosensors for detection of biochemical markers relevant to osteoarthritis," *Biosensors*, Feb. 2021, doi: [10.3390/bios11020031](https://doi.org/10.3390/bios11020031).
- [31] L. Hellweg *et al.*, "A general method for the development of multicolor biosensors with large dynamic ranges," *Nat. Chem. Biol.*, vol. 19, no. 9, pp. 1147–1157, Sep. 2023, doi: [10.1038/s41589-023-01350-1](https://doi.org/10.1038/s41589-023-01350-1).
- [32] D. V. Vokhmyanina, O. E. Sharapova, K. E. Buryanovataya, and A. A. Karyakin, "Novel siloxane derivatives as membrane precursors for lactate oxidase immobilization," *Sensors*, vol. 23, no. 8, Apr. 2023, doi: [10.3390/s23084014](https://doi.org/10.3390/s23084014).
- [33] X. Lin, "Application of biosensors in the detection of plant biomolecules," *Theor. Nat. Sci.*, vol. 23, no. 1, pp. 237–242, Dec. 2023, doi: [10.54254/2753-8818/23/20231072](https://doi.org/10.54254/2753-8818/23/20231072).
- [34] S. Palakurthy, L. Houben, M. Elbaum, and R. Elbaum, "Silica biomineralization with lignin involves Si–O–C bonds that stabilize radicals," *Biomacromolecules*, vol. 25, no. 6, pp. 3409–3419, Jun. 2024, doi: [10.1021/acs.biomac.4c00061](https://doi.org/10.1021/acs.biomac.4c00061).
- [35] K. Maghrebi, S. Gam, B. Hammami, A. Alsadiri, M. Abderrabba, and S. Messaoudi, "Exploration of the mechanism of the dimerization of hydroxymethylsilanetriol using electronic structure methods," *ACS*

- Omega*, vol. 7, no. 3, pp. 2661–2670, Jan. 2022,
doi: [10.1021/acsomega.1c05027](https://doi.org/10.1021/acsomega.1c05027).
- [36] P. Wu et al., “Supporting information: How the Si–O–Si covalent bond interface affects the electrochemical performance of Si anode,” *ACS Appl. Mater. Interfaces*, 2023,
doi: [10.1021/acsaem.2c00747](https://doi.org/10.1021/acsaem.2c00747)
- [37] Z. L. Kong, Y. Liu, and J. H. Jiang, “Topologically integrated photonic biosensor circuits,” *Laser Photonics Rev.*, vol. 19, no. 8, p. 2401209, 2025,
doi: [10.1002/lpor.202401209](https://doi.org/10.1002/lpor.202401209).
- [38] I.J. Leonel, S. Bin Mujib, G. Singh, and A. Navrotsky, “Thermodynamic stabilization of crystalline silicon carbide polymer-derived ceramic fibers,” *Int. J. Ceram. Eng. Sci.*, vol. 4, no. 5, pp. 315–326, Sep. 2022,
doi: [10.1002/ces2.10153](https://doi.org/10.1002/ces2.10153).
- [39] J. Jamoul, S. Smet, S. Radhakrishnan, C. V. Chandran, J. A. Martens, and E. Breynaert, “Polysilicate porous organic polymers (PSiPOPs), a family of porous, ordered 3D reticular materials with polysilicate nodes and organic linkers,” *Chem. Mater.*, vol. 36, no. 3, pp. 1385–1394, 2024,
doi: [10.1021/acs.chemmater.3c02546](https://doi.org/10.1021/acs.chemmater.3c02546).
- [40] I. Zhu, X. Fang, X. Liu, D. Luo, W. Yu, and H. Zhang, “High-rate SiO₂ lithium-ion battery anode enabled by rationally interfacial hybrid encapsulation engineering,” *ACS Appl. Mater. Interfaces*, vol. 16, no. 5, pp. 5915–5925, 2024,
doi: [10.1021/acsaami.3c17064](https://doi.org/10.1021/acsaami.3c17064)
- [41] S. A. Sari and A. N. Sari Lubis, “The development of dusting method for dragon fruit peel as fingerprint visualization,” *JKPK (J. Kim. Pendidik. Kim.)*, vol. 6, no. 1, p. 1, Apr. 2021,
doi: [10.20961/jkpk.v6i1.46315](https://doi.org/10.20961/jkpk.v6i1.46315).
- [42] S. A. Sari, H. Hasibuan, R. M. Siahaan, and N. H. S. Mais, “Biosynthesis and characterization of ZnO nanoparticles with papaya leaf extract (*Carica papaya* L.) as latent fingerprint identification,” in *Proc. Semin. Nas. Kimia*, Surabaya, Sep. 2023, pp. 81–88.
- [43] F. Hameed, A. K. Mohammed, and D. S. Zageer, “Comparative study between activated carbon and charcoal for the development of latent fingerprints on nonporous surfaces,” *Al-Khwarizmi Eng. J.*, vol. 18, no. 4, pp. 1–13, Dec. 2022,
doi: [10.22153/kej.2022.09.001](https://doi.org/10.22153/kej.2022.09.001).
- [44] H. J. A. Yadav, B. Eraiah, M. N. Kalasad, and M. D. Hadagali, “Nanomaterials for forensic applications: A review,” *Int. J. Mater. Manuf. Sustain. Technol.*, pp. 4–11, Sep. 2022,
doi: [10.56896/ijmmst.2022.1.1.002](https://doi.org/10.56896/ijmmst.2022.1.1.002).
- [45] P. Boonyaras, S. Boonpang, and K. Dangudom, “Latent fingerprint detection using fluorescent powder dusting technique,” in *J. Phys. Conf. Ser.*, 2023,
doi: [10.1088/1742-6596/2653/1/012075](https://doi.org/10.1088/1742-6596/2653/1/012075).
- [46] Y. Gülekçi and A. Tülek, “Optimization of crystal violet technique for enhanced fingerprint detection on various surfaces,” *J. Forensic Sci.*, vol. 69, no. 4, pp. 1246–1255, Jul. 2024,
doi: [10.1111/1556-4029.15534](https://doi.org/10.1111/1556-4029.15534).
- [47] S. A. A. Sarifudin, K. H. Chang, C. H. Yew, V. Kunalan, B. E. Khoo, and A. F. L. Abdullah, “Recovery and visualisation of methamphetamine-contaminated fingerprints from non-porous surfaces,” *Malaysian J. Med. Health Sci.*, vol. 19, no. 6, pp. 178–185, Nov. 2023,
doi: [10.47836/mjmh.19.6.24](https://doi.org/10.47836/mjmh.19.6.24).
- [48] J. Parkale and M. S. Bagul, “A review of latent fingerprint developed powder from using natural materials,” *Int. J. Sci. Res. Sci. Technol.*, vol. 11, no. 2, pp. 715–717, Apr. 2024,
doi: [10.32628/ijrsr24112115](https://doi.org/10.32628/ijrsr24112115).

- [49] T. Kobayashi and M. Pruski, "Indirectly detected DNP-enhanced ^{17}O NMR spectroscopy: Observation of non-protonated near-surface oxygen at naturally abundant silica and silica-alumina," *ChemPhysChem*, vol. 22, no. 14, pp. 1441–1445, Jul. 2021, doi: [10.1002/cphc.202100290](https://doi.org/10.1002/cphc.202100290)
- [50] A.M. Jewell *et al.*, "Three North African dust source areas and their geochemical fingerprint," *Earth Planet. Sci. Lett.*, vol. 554, p. 116645, 2021, doi: [10.1016/j.epsl.2020.116645](https://doi.org/10.1016/j.epsl.2020.116645). doi: [10.1016/j.epsl.2020.116645](https://doi.org/10.1016/j.epsl.2020.116645).
- [51] V. Wonoputri, T. W. Samadhi, S. Khairunnisa, and E. Rahayu, "Role of deagglomeration in particle size and antibiofilm activity of ZnO nanoparticles synthesized with *Averrhoa bilimbi* extract," *J. Eng. Technol. Sci.*, vol. 56, no. 6, pp. 727–741, 2024, doi: [10.5614/j.eng.technol.sci.2024.56.6.5](https://doi.org/10.5614/j.eng.technol.sci.2024.56.6.5).
- [52] N. E. A. El-Naggar, S. R. Dalal, A. M. Zweil, and M. Eltarahony, "Artificial intelligence-based optimization for chitosan nanoparticles biosynthesis, characterization and in vitro assessment of its anti-biofilm potentiality," *Sci. Rep.*, vol. 13, no. 1, Dec. 2023, doi: [10.1038/s41598-023-30911-6](https://doi.org/10.1038/s41598-023-30911-6)
- [53] Flieger, W. Flieger, J. Baj, and R. Maciejewski, "Antioxidants: Classification, natural sources, activity/capacity measurements, and usefulness for the synthesis of nanoparticles," *Materials*, Aug. 2021, doi: [10.3390/ma14154135](https://doi.org/10.3390/ma14154135).
- [54] R. L. White, "A temperature perturbation infrared spectroscopy comparison of HY and NaY zeolite dehydration/rehydration," *Minerals*, vol. 14, no. 1, Jan. 2024, doi: [10.3390/min14010104](https://doi.org/10.3390/min14010104).
- [55] Z. Ma, H. Liao, Z. Pan, and F. Cheng, "Insights into coproduction of silica gel via desulfurization of steel slag and silica gel adsorption performance," *ACS Omega*, vol. 7, no. 24, pp. 21062–21074, Jun. 2022, doi: [10.1021/acsomega.2c01857](https://doi.org/10.1021/acsomega.2c01857).
- [56] J. H. Jacobs, K. H. McKelvie, S. Nanji, and R. A. Marriott, "Sour gas adsorption on silica gels," *ACS Omega*, vol. 8, no. 13, pp. 12592–12602, Apr. 2023, doi: [10.1021/acsomega.3c01366](https://doi.org/10.1021/acsomega.3c01366).
- [57] S. A. Yamada, S. T. Hung, J. Yoon Shin, and M. D. Fayer, "Complex formation and dissociation dynamics on amorphous silica surfaces," *J. Phys. Chem. Lett.*, 2023.
- [58] Y. Ikemoto *et al.*, "Infrared spectra and hydrogen-bond configurations of water molecules at the interface of water-insoluble polymers under humidified conditions," *J. Phys. Chem. B*, vol. 126, no. 22, pp. 4143–4151, Jun. 2022, doi: [10.1021/acs.jpcc.2c01702](https://doi.org/10.1021/acs.jpcc.2c01702).
- [59] Y. Xia, C. Calahoo, B. P. Rodrigues, K. Griebenow, L. Graewe, and L. Wondraczek, "Structure and properties of cerium phosphate and silicophosphate glasses," *J. Am. Ceram. Soc.*, vol. 106, no. 5, pp. 2808–2819, May 2023, doi: [10.1111/jace.18936](https://doi.org/10.1111/jace.18936).
- [60] R. G. Schireman, J. Maul, A. Erba, and M. T. Ruggiero, "Anharmonic coupling of stretching vibrations in ice: A periodic VSCF and VCI description," *J. Chem. Theory Comput.*, vol. 18, no. 7, pp. 4428–4437, 2022, doi: [10.1021/acs.jctc.2c00217](https://doi.org/10.1021/acs.jctc.2c00217)
- [61] I. Shi and W. Min, "Vibrational solvatochromism study of the C–H \cdots O improper hydrogen bond," *J. Phys. Chem. B*, vol. 127, no. 17, pp. 3798–3805, 2023, doi: [10.1021/acs.jpcc.2c08119](https://doi.org/10.1021/acs.jpcc.2c08119).
- [62] S. N. Matussin *et al.*, " α -Glucosidase inhibitory activity and cytotoxicity of

- CeO₂ nanoparticles fabricated using a mixture of different cerium precursors," *ACS Omega*, vol. 9, no. 1, pp. 157–165, Jan. 2024, doi: [10.1021/acsomega.3c02524](https://doi.org/10.1021/acsomega.3c02524).
- [63] B. Xu *et al.*, "Clinical characteristics and early prediction of mortality risk in patients with acute organophosphate poisoning-induced shock," *Front. Med.*, vol. 9, p. 990934, 2023, doi: [10.3389/fmed.2022.990934](https://doi.org/10.3389/fmed.2022.990934).
- [64] X. Yao *et al.*, "Interfacial properties of the nitrogen + water system in the presence of hydrophilic silica," *Ind. Eng. Chem. Res.*, vol. 63, no. 13, pp. 5765–5772, Apr. 2024, doi: [10.1021/acs.iecr.3c04541](https://doi.org/10.1021/acs.iecr.3c04541).
- [65] I.M. Islam *et al.*, "Facile fabrication and characterization of amine-functional silica coated magnetic iron oxide nanoparticles for aqueous carbon dioxide adsorption," *ACS Omega*, vol. 9, no. 19, pp. 20891–20905, May 2024, doi: [10.1021/acsomega.3c10082](https://doi.org/10.1021/acsomega.3c10082).